STUDIA UBB CHEMIA, LXVIII, 2, 2023 (p. 169-184)
(RECOMMENDED CITATION)
DOI:10.24193/subbchem.2023.2.11

# DISPERSION IN A TWO-PHASE FLOW SULZER COLUMN

**Eugenia Teodora IACOB TUDOSE**[a]

**ABSTRACT.** An experimental study based on the pulse-response technique was performed in a Sulzer packed-bed column in order to establish the residence time distribution for four different liquid flow rates, namely 200, 400, 600 and 800 L/h and five different gas flow rates of 0, 5, 10, 15, 20 $m^3$/h. Depending on the phase flow rate, comparisons with the axial distribution and the N-tanks–in–series models rendered good similarities. Furthermore, the axial dispersion coefficient and its dependence on the superficial velocity of the liquid phase, for various gas flow rates and also, on the F factor of the gas phase, for various liquid flow rates, have been established.

***Keywords:*** *Sulzer column, axial dispersion, residence time distribution, dispersion model, cellular model*

## INTRODUCTION

Axial dispersion is an important parameter that affects the performance of fixed-bed columns, so the literature indicates a large number of theoretical and experimental studies on the subject [1-5].

The current study was initiated to characterize the hydrodynamics of two-phase flows in a Sulzer packed column and to investigate the differential models usable for various flow rates of the two phases, gas and liquid, to approximate significant deviations from idealized total displacement flow.

The pulse-response technique [6] was used to obtain the residence time distribution in a Sulzer column. It consists of injecting a chemical inert tracer (sodium chloride) in the water stream feeding the column and

[a] *"Cristofor Simionescu" Faculty of Chemical Engineering and Environmental Protection, "Gheorghe Asachi" Technical University, 73 Bd. Prof. Dr Doc. Dimitrie Mageron, RO-700050, Iaşi, Romania, etudose@tuiasi.ro; eugenia.iacob2017@gmail.com*

recording the tracer concentration signal, at the column exit, using a conductometer, previously calibrated for NaCl solutions, of different concentrations.

The diffusion equation for the tracer used flowing through the column is:

$$\frac{\partial c}{\partial t} = D\frac{\partial^2 c}{\partial z^2} \pm u\frac{\partial c}{\partial z} \tag{1}$$

Using some initial and boundary conditions:

$$t = 0,\ 0 < z < L,\ \ c = 0 \tag{2}$$

$$t = 0,\ z\ = 0,\ c_0 u = cu - D\frac{\partial c}{\partial z} \tag{3}$$

$$t > 0,\ z = L,\ \frac{\partial c}{\partial z} = 0 \tag{4}$$

and solving the above Eq.(1), the normalized residence time distribution function E(θ) for the dispersion axial model in a closed system is obtained in the form [7,8]:

$$E(\theta) = \exp\left(\frac{Pe}{2}\right)\sum_{j=1}^{\infty}\frac{(-1)^{j+1}8\alpha_j^2}{4\alpha_j^2 + 4Pe + Pe^2 exp}exp\left[-\frac{4\alpha_j^2 + Pe^2}{4Pe}\theta\right] \tag{5}$$

where αj are the positive roots of the following equation:

$$tg\alpha_j = \frac{4Pe\alpha_j}{4\alpha_j^2 - Pe^2} \tag{6}$$

with Pe the liquid phase Péclet number [7] and the normalized variance, $\sigma_\theta^2$, given by [7,8]:

$$\sigma_\theta^2 = \frac{2}{Pe_L} - \frac{2}{Pe_L^2}[1 - exp(-Pe_L)] \tag{7}$$

equation that can be simplified for large Pe values to:

$$\sigma_\theta^2 = \frac{2}{Pe_L} \tag{8}$$

Based on the experimental value $\sigma_\theta^2$, using Eq.(8), one can calculate the Pe number.

It is known that for large Pe numbers (Pe≥25, the closed and open system axial dispersion distributions, E(θ), are almost identical [7] and the distribution function for an open system is given by:

$$E(\theta) = \sqrt{\frac{Pe_L}{4\pi\theta}} exp\left[-\frac{Pe_L(1-\theta)^2}{4\theta}\right] \quad (9)$$

Another model used to describe the residence time distribution in a column is the cellular model. This is a discrete model that considers the axial mixing of the liquid or gas phases by means of a series of elements (usually of constant volume) interconnected through the main convective flow, elements in which the mixing is perfect. The degree of mixing is characterized by the number of perfectly mixed cells. For a sufficiently large deviation from the ideal case of perfect mixing, the model can be considered to be equivalent to the axial dispersion model. So, N=1 corresponds to a perfectly mixed flow, N=∞ corresponds to flow with total displacement. For the cellular model, the distribution function of stationary times, dimensional and nondimensional, follows the equations [7]:

$$E(t) = \frac{C(t)}{\int_0^\infty C(t)dt} = \frac{t^{N-1}}{(N-1)\tau_i^N} e^{-\frac{t}{\tau_i}} \quad (10)$$

$$E(\theta) = \tau E(t) = \frac{N(N\theta)^{N-1}}{(N-1)!} e^{-N\theta} \quad (11)$$

where *N* is the cell number, $\tau_i$ is the residence time in cell *i*, the dispersion, $\sigma_\theta^2$, can be used to determine the number of cells necessary to obtain the same degree of mixing as in the column:

$$N = 1/\sigma_\theta^2 \quad (12)$$

## RESULTS AND DISCUSSION

The conductance experimental data were analyzed in Excel files and graphically represented to underline the liquid flowrate influence on the residence time distribution and finally, on the axial dispersion, at different constant gas flowrates.

Comparison with the above-mentioned models of residence time distribution highlights the extent to which these could be used, in certain value ranges of the investigated parameters. Also, the dispersion coefficient in the column was calculated based on the studied parameters.

**Influence of the fluid flowrate on the residence time distribution**

The experimental concentration data have been used to calculate respectively, the residence time distribution function, E(t), the normalized residence time distribution function, E(θ), the mean residence time, $\tau$, the normalized mean residence time, θ, the variance, $\sigma^2$, and the normalized variance, $\sigma_\theta^2$, based on the following equations [8]:

$$E(t) = \frac{C(t)}{\int_0^\infty C(t)dt} \quad (13) \qquad E(\theta) = \tau E(t) \quad (14)$$

$$\tau = \frac{\sum t_i C_i \Delta t_i}{\sum C_i \Delta t_i} \quad (15) \qquad \theta = \frac{t_i}{\tau} \quad (16)$$

$$\sigma^2 = \frac{\int_0^\infty t^2 cdt}{\int_0^\infty cdt} - \tau^2 \quad (17) \qquad \sigma_\theta^2 = \frac{\sigma^2}{\tau^2} \quad (18)$$

**Liquid-phase flow through the column**

The experiments were conducted in the Sulzer column fed at water flowrates of 200, 400, 600 and 800 L/h. Based on the measured concentrations, the normalized residence time distribution functions, E(θ), as a function of the normalized mean residence time, θ, for different liquid flowrates, were determined and represented in Figure 1.

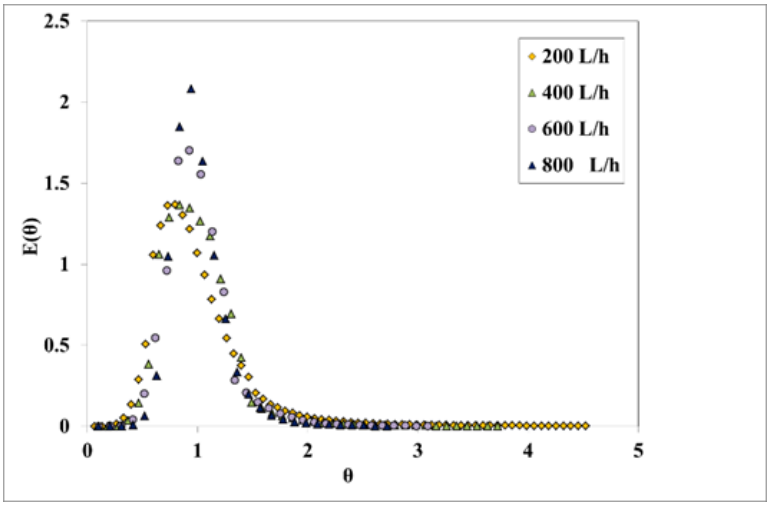


**Figure 1.** Distribution of the normalized residence time distribution as a function of the normalized mean residence time, for different liquid flowrates (single-phase flow - liquid)

One can observe that all distributions have an almost symmetrical profile, with a maximum near the value θ = 1. For most of the graphs, the maximum distribution function E(θ) corresponds to a value θ<1, which suggests the existence of regions with somewhat preferential flow inside the column.

As the liquid flowrate increases, higher residence time distributions are recorded experimentally, a calculation of the normalized dispersion, based on equation (15), indicating lower values which translates in a reduction of the axial dispersion, thus a flow closer to the plug flow.

### Gas-liquid flow through the column

When both gas and liquid phases were fed countercurrently in the Sulzer column, the residence time distribution had similar trends to the ones obtained for the single liquid phase flow, corresponding to an axial dispersion decrease, when the liquid flowrate increases from 200 L/h to 800 L/h, at each investigated gas flow rate, kept constant, at 5, 10, 15 and 20 $m^3$/h respectively, data shown in Figure 2 (a) - (d), respectively.

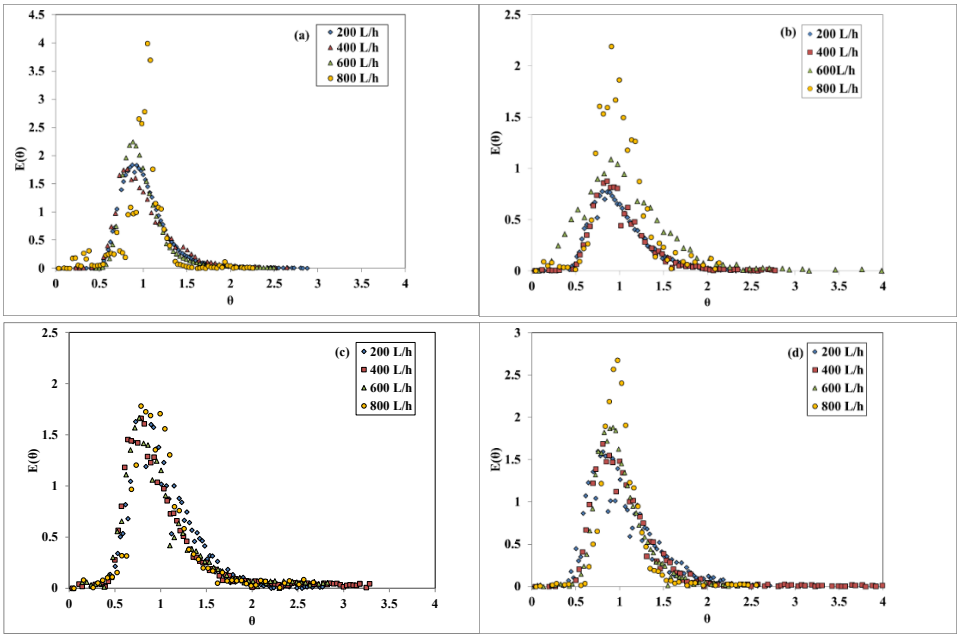


**Figure 2.** Distribution of the normalized residence time distribution as a function of the normalized mean residence time, for different liquid flowrates, at constant gas flowrate (a) 5$m^3$/h, (b) 10$m^3$/h, (c) 15$m^3$/h, (d) 20 $m^3$/h (two-phase flow)

In each graphical representation, there is an increase in the experimental data's dispersion, with an increase of the liquid flowrate, at a constant gas flowrate, which indicates the non-uniformities of the liquid phase flow, especially at high flow rates of 800 L/h.

In addition, comparison of Figures 2 a) with b), c) and especially, d) shows that the experimental points distribution increases with the increase of the circulating gas flow, which indicates the occurrence of more uneven convection areas inside the column, although the distribution preserves the general approximately symmetrical shape around θ = 1.

**Comparison with residence time distribution models**

The experimental residence time distribution may or may not be similar to the theoretical distributions established by other models mentioned in Introductory part, namely, the axial dispersion and the cellular models. The degree to which the experimental data approaches one of the mentioned models indicates to what extent dispersion occurs in the column.

For the dispersion model, starting from the experimental value of the normalized dispersion, $\sigma_\theta^2$, firstly the Peclet number of the liquid phase was calculated using equation (8) and afterwards, the normalized distribution of the residence times E(θ)_disp using equation (9) in order to be compared with the distribution function obtained experimentally, E(θ)_exp.

For the cellular model, starting from the experimental values of the normalized dispersion, $\sigma_\theta^2$, the number of N cells was calculated using equation (12), and subsequently, using equation (11), the residence time distribution function, E(θ)_cel, for comparison with the distribution function obtained experimentally, E(θ)_exp.

In Figures 3 (a) - (d) the distributions of the residence time distributions obtained experimentally and those calculated, corresponding to the two models, of axial and cellular dispersions, respectively, were represented for different flow rates of liquid and gas, maintained at constant values. .

It can be observed that at small liquid flow rates of 200 L/h, in the absence of gas supply (gas flow 0 $m^3$/h), the distribution of the residence times is different from that of the cellular model or the axial dispersion models, as seen in Figure 3 (a). One possible explanation is the small amount of fluid flow that probably has a preferential path through the fixed bed.

Comparison of the experimental data with the cellular model is not verified even when increasing the liquid flow to values of 400 L/h, 600 L/h and, respectively, 800 L/h, gas flow 0 $m^3$/h, on the other hand, a good agreement can be observed with the axial dispersion model, according to

Figure 3 (b), (c) and, respectively, (d), a fact consistent with Levenspiel's recommendation to use the axial dispersion model in the field of Péclet numbers Pé>1 [9], in the mentioned domain, the numbers Pé having values between 18.85 and 34.38.

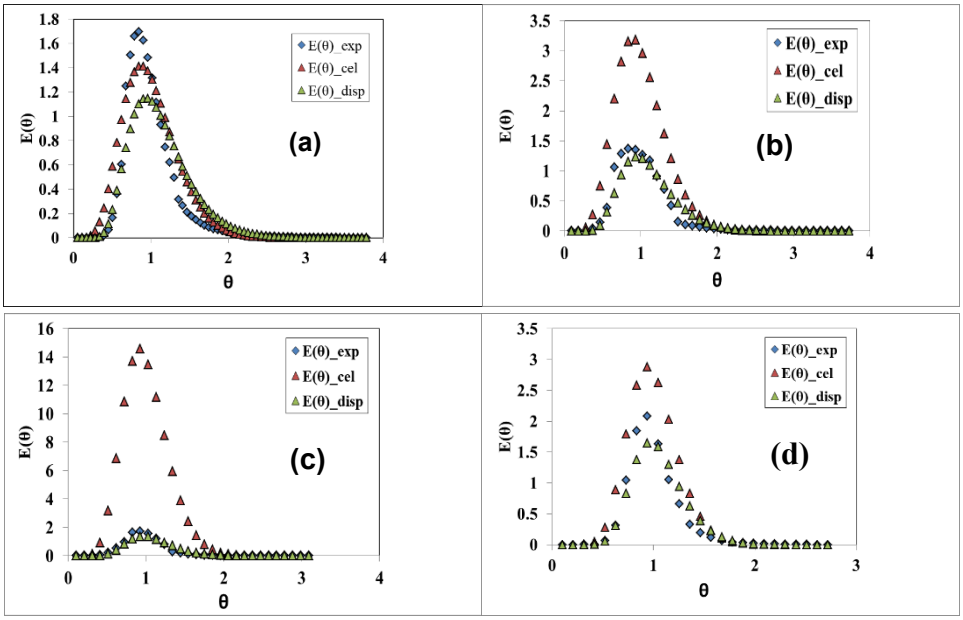


**Figure 3**. Residence time distribution, at a 0 $m^3/h$ gas flowrate and different liquid flowrates: **a)** 200 L/h; **b)** 400 L/h; **c)** 600 L/h; **d)** 800 L/h

At small values of gas flow of 5 $m^3/h$ and small liquid flow rates of 200 L/h, the distribution of the residence times obtained experimentally is practically identical to that of the axial dispersion and the cellular models, according to Figure 4(a). As the liquid flow rate increases, at the same gas flow rate of 5 $m^3/h$, reasonably good agreement between the distribution of the residence times obtained from experimental data and the axial dispersion model, as seen in Figures 4(b)-(d). However, in the same figures, an increasing deviation from the experimental data corresponding to the cellular model is registered. The difference between the cellular model and the experimental data can be explained by the fact that in the column there are preferential flows that intensify when liquid flow rates increase, thus the axial dispersion increases. As a result, the number of N cells becomes larger, which will determine larger E(θ)_cel values in comparison to those obtained experimentally, E(θ) _exp.

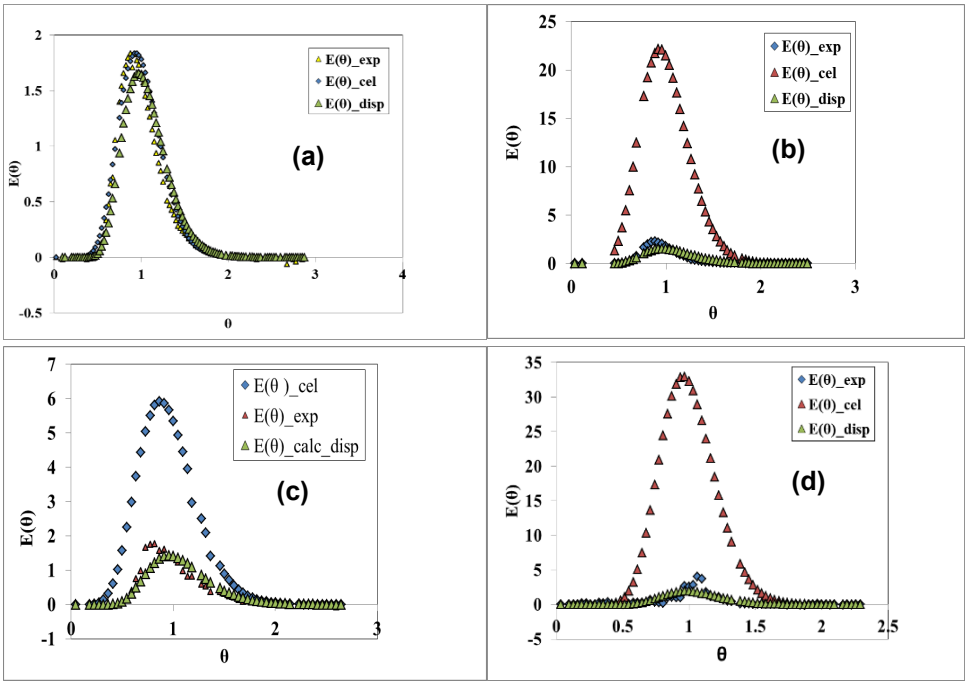


**Figure 4.** Residence time distribution, at a 5 m3/h gas flowrate and different liquid flowrates: **a)** 200 L/h; **b)** 400 L/h; **c)** 600 L/h; **d)** 800 L/h

In Figure 5 (a) – (d) the distributions of the residence times, at a constant gas flow of 10 $m^3$/h and different liquid flow rates, are represented. The graphs in Figure 5 (a) and (b), respectively, for liquid flow rates of 200 L/h and 400 L/h respectively, indicate a certain similarity with the axial dispersion model, although the experimental data show a maximum at θ <1, suggesting the existence of preferential flows, while for larger flow rates of 600 L/h and 800 L/h respectively, the distributions of the residence times are similar to the calculated axial dispersion model distributions, as shown in Figure 6 (c) and (d), indicating a more efficient spreading of the liquid phase along the column. Again, the cellular model data are much different when compared to the experimental data.

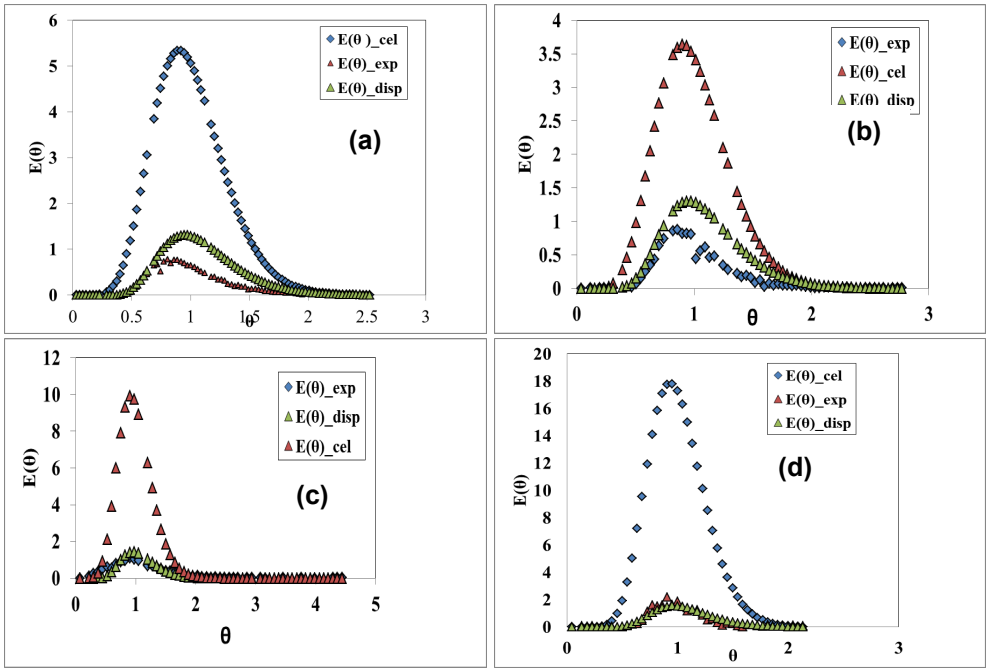


**Figure 5**. Residence time distribution, at a 10 $m^3$/h gas flowrate and different liquid flowrates: **a)** 200 L/h; **b)** 400 L/h; **c)** 600 L/h; **d)** 800 L/h

In Figure 6(a) – (d), the residence time distribution, at a constant gas flow rate of 15 $m^3$/h and different liquid flow rates, indicate different results. For liquid flow rates of 200 L/h, as seen in Figure 6(a), similarities between the experimental data and the axial dispersion model are observed, with some preferential flows, while for liquid flow rates of 600 L/h and 800 L/h respectively, the graphs in Figure 6 (c) and (d) respectively, indicate similar residence time distributions for the experimental and the cellular model data. However, the dispersion in the two cases is to some extent different, the one corresponding to the experimental data being smaller, fact indicating a flow regime with a more significant total displacement of the liquid in the column. At a fluid flow rate of 400 L/h, at the same gas flow of 15 $m^3$/h, none of the models is likely to be checked due to the occurrence of partial bed flooding.

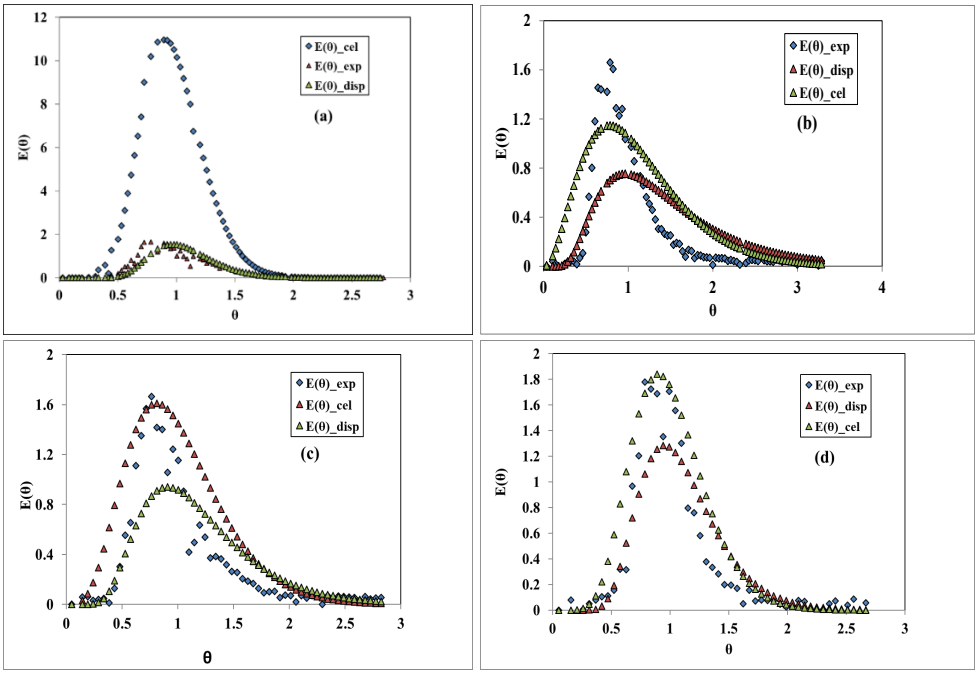


**Figure 6**. Residence time distribution, at a 15 $m^3$/h gas flowrate and different liquid flowrates: **a)** 200 L/h; **b)** 400 L/h; **c)** 600 L/h; **d)** 800 L/h

Figures 7 (a) – (d) containing the same type of distributions at a constant air flow rate of 20 $m^3$/h and liquid flow rates of 200 L/h, 400 L/h, 600 L/h and 800 L/h, respectively, indicate that the experimental data are similar to the axial dispersion model data, however they are very different from the cellular model values, for all investigated parameters values. Although the cellular model values were compared with the experimental data for all cases, the former ones are included only in Figure 7(a) and omitted in Figure 7 (b)-(d), in order to better highlight the eventual similarity of the experimental data to the RTDs corresponding to the axial dispersion model.

The measured values displayed in Figure 7 (a) are more dispersed in comparison to the axial dispersion values, probably due to the small liquid flow rate associated with the high gas flow rate, throughout the column. In Figure 7 (b) and (c), one notices some differences between the distribution of the experimental data and those of the axial dispersion model, this may be due to the occurrence of column partial flooding phenomenon, at flow rates slightly greater than 200 L/h and a gas flow rate of 20 $m^3$/h.

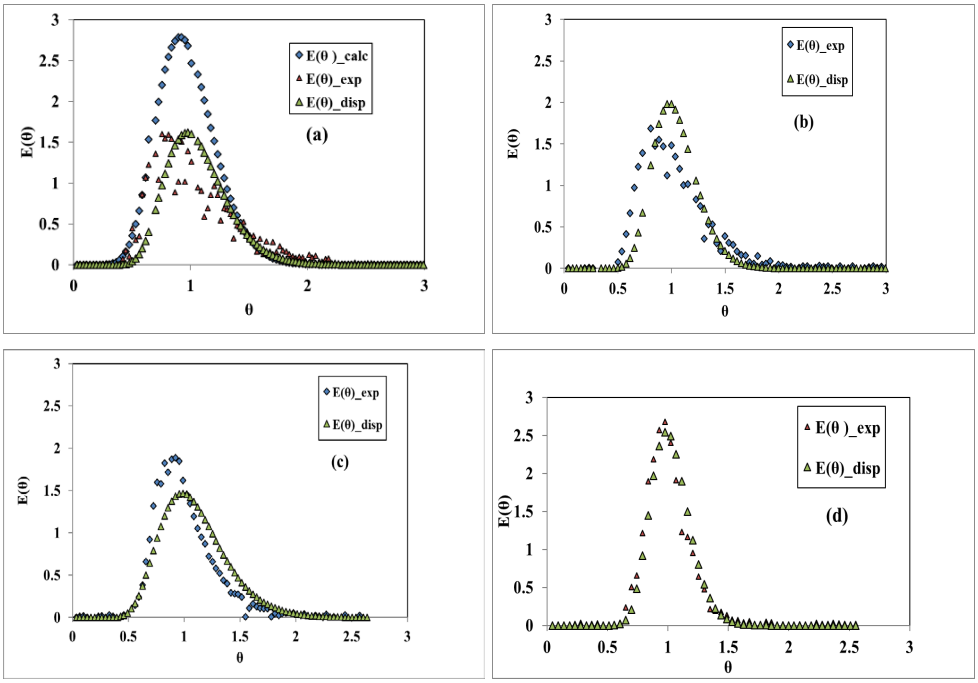


**Figure 7**. Residence time distribution, at a 20 $m^3$/h gas flowrate and different liquid flowrates: **a)** 200 L/h; **b)** 400 L/h; **c)** 600 L/h; **d)** 800 L/h

At a liquid flow rate greater than 800 L/h, the gas phase no longer sustains the liquid phase flow, and the agreement of the experimental data with the axial dispersion model appears again.

A systematization of the verified models for certain gas and liquid flow rates, on the Sulzer packings filled column, is presented in Table 1:

**Table 1.** Distribution of residence times according to a certain model, the axial dispersion model (DM) and/or the cellular model (CM), depending on the value of the liquid and gas flow rates in the Sulzer column, with $M_{m,l}$ the liquid flow rate and $M_{m,g}$ the gas flow rate.

| **$M_{m,l}$ (L/h)** **$M_{m,g}$ ($m^3$/h)** | **200** | **400** | **600** | **800** |
|---|---|---|---|---|
| **0** | CM | DM | DM | ~DM |
| **5** | CM/DM | DM | DM | DM |
| **10** | ≈ DM | ≈ DM | DM | DM / |
| **15** | DM | partially flooded | partially flooded | partially flooded |
| **20** | DM / partially flooded | partially flooded | partially flooded | DM |

The following two figures, 8 and 9, illustrate the gas liquid flow in the Sulzer column, for normal flow conditions and partially flooded packings, respectively.

**Figure 8.** Normal gas-liquid flow conditions in a 9 Sulzer packed column (gas flow rate = 5 $m^3$/h and liquid flow rate = 800 L/h)

**Figure 9.** Partially flooded Sulzer packed column (gas flow rate = 20 $m^3$/h and liquid flow rate = 200 L/h)

**Estimation of the dispersion coefficient from RTD distributions**

An estimate of the dispersion coefficient from the dispersion values determined from the graphs of the distribution functions of the stationary times obtained experimentally, according to the equation [7]:

$$\frac{D}{u_L H} = \frac{\sigma_\theta^2}{2} \tag{19}$$

where $D$ is the axial dispersion coefficient, $u_L$ is the surface velocity of the liquid phase through the column, $H$ is the height of the Sulzer bed. Graphical representations of the dispersion coefficient as a function of the liquid superficial velocity of the liquid phase, at various flow rates of the gas phase, are shown in Figure 10 (a) and indicate its direct proportional increase. As the flow rate of gas flowing counter-currently through the column increases, the dispersion coefficient decreases. The variation of the dispersion coefficient with the surface velocity of the liquid phase agrees with other results in the literature [10, 11].

In Figure 10(b), the axial dispersion coefficient, D, is represented, as a function of the factor F of the gas phase calculated with the equation:

$$F = u_g \sqrt{\rho_g} \tag{20}$$

where $u_g$ is the gas phase superficial velocity and $\rho_g$ is the gas phase density at an average column temperature. It is observed that the value of the dispersion coefficient is almost independent on the gas phase F factor, as indicated by other data in the literature for different types of packings. The values of the dispersion coefficients were not represented for the parameters at which column flooding occurs.

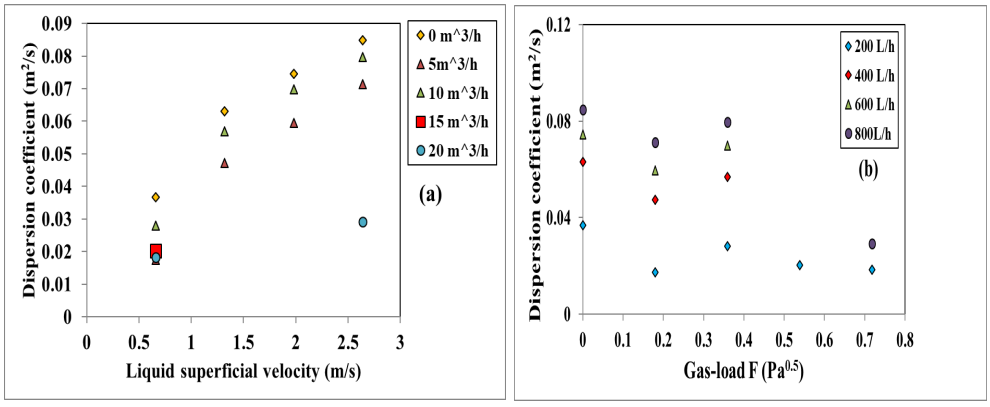


**Figure 10.** Variation of the dispersion coefficient, D, with:
(a) the superficial velocity of the liquid phase, for various gas flow rates;
(b) the F factor of the gas phase, for various liquid flow rates

## CONCLUSIONS

The impulse-response technique used in this experimental study proved to be a sufficiently accurate method to establish the variation trends of some important quantities in the operation of Sulzer packed columns, depending on the working parameters.

In conclusion, at small liquid flow rates of 200 L/h, in the absence of gas phase circulation, but also, at small gas flow rates of 5 $m^3$/h, the distribution of residence times respects the cellular model distribution, in contrast, at higher gas flow rates, of 10 $m^3$/h, for all the investigated liquid flow rates of 200 L/h, 400 L/h, 600 L/h, and 800 L/h, the distributions of the residence times are similar to those calculated using the axial dispersion model. The experimental distributions obtained for a gas flow of 15 $m^3$/h, at a liquid flow of 200 L/h, respect the axial dispersion model, but this is no longer verified at higher flow rates of liquid of 400 L/h, 600 L/h and 800 L/h, a possible explanation being the occurrence of column partial flooding that appears for the mentioned operating conditions. At an air flow of 20 $m^3$/h, the distribution of the residence times is in accordance with the distribution of the axial dispersion model for a liquid flow of 200L/h, but with the increase of the liquid flow at 400 L/h and 600 L/h, the column is partially flooded and none of the investigated models are verified. At an increase of the liquid phase flow at 800 L/h, the column flooding is practically diminished, and the axial dispersion pattern is regained.

## EXPERIMENTAL SECTION

The experimental set-up was used to determine the residence time distribution and the axial dispersion coefficient in a liquid and respectively, a gas-liquid flow column with structured packings.

The experimental setup, shown in Figure 11, includes a fixed bed column (1), filled with Sulzer packages, a centrifugal ventilator (2), an air flowmeter (3), a liquid rotameter (4), a conductometer probe (5) connected to a WTW 315i conductometer (6) to record the exit concentration of the liquid salt injected at the column top, a collecting tank (7) and digital thermometers (8) to measure both inlet and outlet, gas and liquid temperatures.

The column (1) has an inside diameter of 10.35 cm and contains nine Sulzer packages, interspaced with thin annular-shaped redistributors to allow an even liquid spreading across the column cross-sectional area. The column total height is 1.2 m and the structured packed zone is 0.9 m height.

All the experiments have been conducted at room temperature (~20°C), for different water flowrates of 200, 400, 600 and 800 L/h and gas flowrates of 0, 5, 10, 15, 20 $m^3/h$.

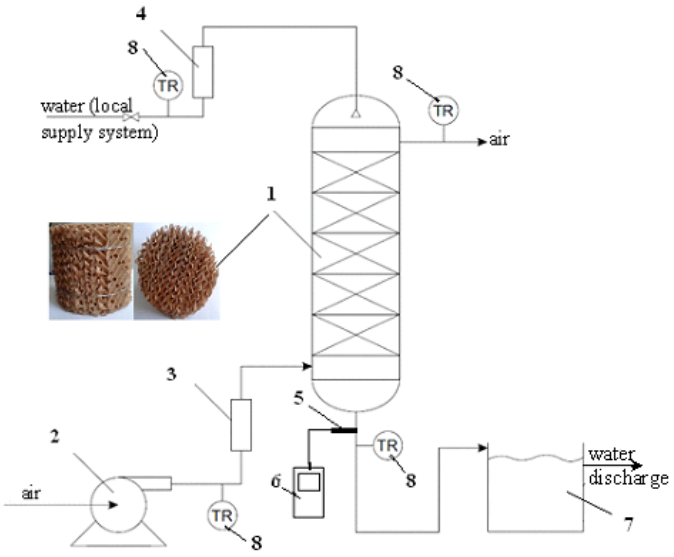


**Figure 11.** Sketch of an experimental setup with a Sulzer column:
1 - Sulzer column (detail: one Sulzer package); 2-centrifugal ventilator;
3-air flowmeter 4- liquid flowameter, 5 – conductometer probe;
6-conductometer, 7-vessel; 8-digital thermometers.

The pulse-response technique used to obtain experimentally the residence time distribution function consisted of injecting 20 mL 10% mass concentration NaCl solution in a pulsed signal, at the upper part of the column, at the liquid entrance. At the same time, the conductometer response signal was monitored in time in order to register the NaCl concentration variation in the liquid phase, at the column outlet. Based on the calibration curve previously obtained, the sodium chloride concentrations, at the column exit, were obtained.

The Sulzer type structured packing is characterized by a large contact area, consisting of layers of wire mesh, with descending channels towards left or right, which ensures basically complete wetting of the surface by the liquid phase through adhesion and capillary forces, subsequently inducing an increased intensity of the property transfers [12, 13]. The Sulzer packages used in these experiments are made of phosphor bronze mesh with the following characteristics: specific surface $1650 m^2/m^3$, void fraction 0.13 $m^3/m^3$, specific mass $430 kg/m^3$. Other construction features can be found in reference [14].

For each experiment, the salt concentration variation at the column exit for subsequent residence time calculations was recorded (data acquisition frequency 1 Hz) using a WTW 315i conductometer, previously calibrated with standard NaCl solutions.

Subsequently, to verify the experimental trends, tests using solutions of NaCl 20% mass concentration, were repeated in the same operating conditions.

## REFERENCES


1. E.Tsotsas; E.U.Schlünder, *Chem. Eng. Proc*., **1998**, *24(1)*, 15-31.
2. K.D.P.Nigham; I.Iliuță; F.Larachi, *Chem.Eng. Proc.,* **2002**, *41*, 365-371.
3. S.Perrin; S.Chaudourne; C.Jallut; J.Lieto, *Chem.Eng.Sc.*, **2002**, *57*, 3335-3345.
4. J.M.P.Q.Delgado, *Chem.Eng. Res. Des*., **2007**, *85(19)*, 279-310.
5. M.Popa; I.Mămăligă,S; Petrescu; E.T. Iacob Tudose, *Revista de chimie*, **2015,** *66(5*), 668-672.
6. A.E.Rodrigues, *Chem. Eng. Sci.*, **2021**, *230*, 116188.
7. G.Bozga; O.Muntean, *Reactoare chimice*, vol. I, *Reactoare omogene*, Ed. Tehnică, București, **2000**, pp.170-171.
8. J.M. Coulson; J.F. Richardson, *Chemical Engineering*, 3, Elsevier Butterworth-Heinemann, Oxford, UK, **2007**, pp.90.
9. O.Levenspiel, *Chemical Reaction Engineering*, 3rd Edition, John Wiley & Sons, New York, **1999**, pp.259-260.
10. J.F Richardson; D.G. Peacock, *Chemical Engineering*, Vol.3, Prentice Hall, London, **1994**.
11. B.S. Abdulrazzaq; *DJES*, **2010**, *03(02)*, 97-112.
12. T.Čmelíková; L.Valenz; E. Lyko Vachková; F.J. Rejl, *Chem. Eng. Res. Design*, **2021**, *172*, pp.175-185.
13. F.J. Rejl; J.Haidl; L. Valenz; A. Marchi; T. Moucha; R. Petříček, E. Brunnazzi, *Chem. Eng. Res. Design*, **2017**, *172*, pp.1-9.
14. I.Ștefănescu; M. Peculea; G.Țițescu, Brevet de invenție B 01 D 59/00, RO-BOPI 8/1998.